

# Improvement of CIGS microstructure and its effect on the conversion efficiency of CIGS solar cells

Ki Hwan Kim<sup>1</sup>, Min Sik Kim<sup>1</sup>, Byung Tae Ahn<sup>1</sup>, Jae Ho Yun<sup>2</sup>, Kyung Hoon Yoon<sup>2</sup>

<sup>1</sup>Department of Materials Science and Engineering, Korea Advanced Institute of Science and Technology, 373-1 Guseong-dong, Yuseong-gu, Daejeon 305-701, Korea

<sup>2</sup>Solar Cells Research Group, Korea Institute of Energy Research, 71-2, Jang-dong, Yuseong-gu, Daejeon, 305-343, South Korea.

Corresponding E-mail: btahn@kaist.ac.kr, y-kh@kier.re.kr

## ABSTRACTS

The Cu(In,Ga)Se<sub>2</sub>(CIGS) film was deposited on Mo-coated sodalime glass by three stage co-evaporation of elemental In, Ga, Cu, and Se sources. The Se flux during the co-evaporation has great influence on the microstructure of CIGS layer. The surface region of CIGS film showed pores when the Se flux was large. The conversion efficiency of CdS/CIGS solar cells was depended on the CIGS surface morphology. The best CIGS solar cell was obtained at 15 Å/s Se vapor pressure condition and it had the following photovoltaic parameters: conversion efficiency of 17.57%, J<sub>sc</sub> = 36.48 mA/cm<sup>2</sup>, Voc = 0.655 V and FF = 73.5% in an active area of 0.421 cm<sup>2</sup>.

## INTRODUCTION

Cu(In,Ga)Se<sub>2</sub>(CIGS) and related chalcopyrite compounds are greatly gaining interest for photovoltaic devices since its high optical absorption coefficient and easy band gap adjustment enable to get cost-effective thin-film solar cell. And very high efficiencies with 19.5% have been achieved by NREL group using three-stage process [1].

In this study, the effect of Se flux during the third-stage co-evaporation on the microstructure of CIGS thin film was systematically studied. The CIGS films were fabricated using three-stage process with *in-situ* composition monitoring by means of sensing the substrate temperature[2]. In order to improve the surface morphology of CIGS films, we controlled the Se flux by regulating the effusion cell temperature. It is known that high Se flux is needed to obtain high conversion efficiency[3]. However, our finding is that a precise

control of Se flux is critical to obtain a reproducible and high conversion efficiency.

## EXPERIMENTAL

A Mo back contact with a thickness 1.1 ~ 1.2 μm was deposited on a soda-lime glass substrate by DC magnetron sputtering. The CIGS absorber layer was grown by a three-stage process involving the co-evaporation of In, Ga, Cu and Se. In the first stage, an (In,Ga)<sub>2</sub>Se<sub>3</sub> layer with a thickness of 1 μm was grown by co-evaporating In, Ga, and Se elements on the Mo/Glass substrates at 350°C. In the second stage, a CIGS film was formed by evaporating Cu and Se on the (In,Ga)<sub>2</sub>Se<sub>3</sub> layer at 590 °C. The end of the second stage was detected by measuring the substrate temperature drop[2]. After the second stage, the overall composition is known to be Cu rich. Since only Cu and Se are supplied during the second stage, the surface region contains a small amount of Cu<sub>2-x</sub>Se[4~8]. In the third stage, In, Ga, and Se elements were evaporated on the CIGS layer in order to convert Cu-poor CIGS film. The final composition was adjusted as Cu<sub>0.9</sub>(In<sub>0.7</sub>,Ga<sub>0.3</sub>)Se<sub>2.1</sub>, where the cation compositions are determined from an EDS analysis and the Se composition is the balance value of cation valences.

In order to investigate the role of Se flux during CIGS deposition, Se flux was regulated by effusion cell temperature ranging from 250 to 285 °C. The selected values of Se flux are 10, 15, 23, and 35 Å/s. The fluxes of In, Ga, and Cu were fixed at a rate of 4.2, 0.7, and 0.9 Å/s, respectively.

## RESULTS and DISCUSSION

Figure 1 shows the SEM images of CIGS film after 3<sup>rd</sup> stage ranging from 15 Å/s and 35 Å/s Se fluxes. After

the second stage, there is no noticeable difference in surface morphology by the same as “facet” shape. However, it is found that the CIGS films exhibit different morphologies by Se fluxes after the third stage, especially. When the Se flux is below 15 Å/s, the film surfaces exhibit tightly connected structure and “facet shape” structure. Fig. 1(c,d) shows that the surface morphology of CIGS film shows crevices and small pits on smooth surface with also “facet” shape structure with the Se flux with 23 Å/s or over.

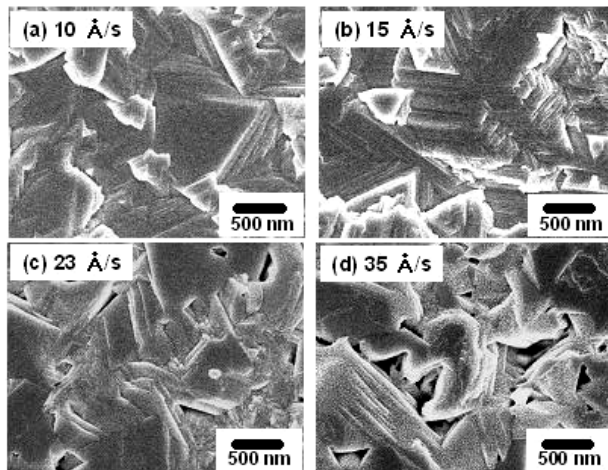


**Fig. 1.** Plane view SEM images of CIGS thin-film with Se vapor pressures ranging from 10 to 35 Å/s during deposition.

The orientation of the faceted grains shown in Fig. 1d and their growth direction are useful information. Figure 2 shows (a) a TEM image and (b) selected area diffraction pattern (SADP) of a faceted CIGS grain with pores. The SADP is obtained from a triangle-shaped grain and it shows that the orientation of the faceted grains is (112) plane, which is equivalent to the (111) plane in cubic ZnS, and the three-fold ledges consist of (220) and (204) plane families.

The origin of faceted grain growth and pore development shown in Fig. 2 can be explained based on the liquid formation at the CIGS surface. After the second stage, the overall composition is Cu-rich and, in particular,  $\text{Cu}_{2-x}\text{Se}$  phase exists on the CIGS surface [4~6]. J. Kessler et al. reported that segregation of  $\text{Cu}_{2-x}\text{Se}$  binary phase play an important role in the formation of pore in the CIGS grain boundaries [9]. However, in our study, it was found that Se flux also has great importance on the formation of pores from the Cu-rich CIGS film. This is expected because Cu and Se are co-evaporated during the second stage. When the Se flux is small, it is expected that the amount of liquid will be small. In and Ga atoms are simultaneously added during the third stage and the liquid

is completely consumed to form (112) CIGS with faceted growth. When the Se flux is large, the amount of liquid is expected to be large. In addition to CIGS growth from co-evaporated In and Ga, CIGS can grow by both the dissolution of In and Ga from neighboring grains and precipitation of the melt constituents onto larger grains through liquid-enhanced long-range diffusion. These result in large grains and the development of pores at the CIGS surface. Pores are mostly formed along the grain boundaries, likely due to higher solubility in these regions.

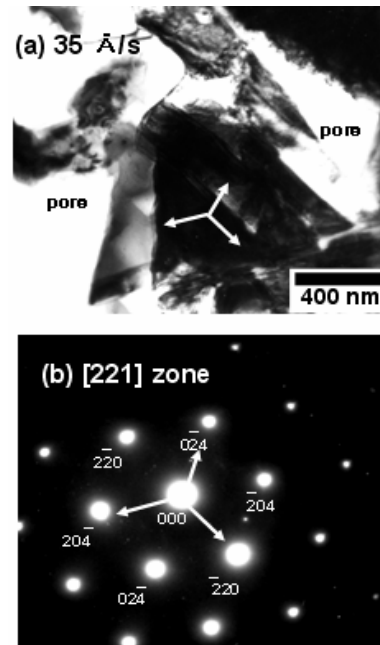


**Fig. 2.** Plane-view TEM image (a) and its SADP (b) of CIGS film with Se flux of 15 Å/s. The faceted structure with pores is shown in (a).

Figure 3 shows the peak intensity ratio of (112)/(220)(204) planes with various incident angles for the CIGS film after the third stage. The x-ray beam incident conditions were bulk ( $\theta$ - $2\theta$  scan,  $2^\circ$  beam angle ( $2\theta$  scan), and  $0.05^\circ$  beam angle (GI-XRD). In the bulk XRD scan, the intensity ratio of the CIGS film is in the range of 22 to 25, indicating that the CIGS bulk film has a very strong (112) preferred orientation. The value is quite similar to that after the second stage. It can be considered that the bulk microstructure does not significantly change after the third stage process.

In the  $2^\circ$  scan, the intensity ratio for the Se flux of 35 Å/s is 5, while that for the Se flux of 15 Å/s Se is 14. This indicates that the CIGS film under the Se flux of 35 Å/s loses its (112) preferred orientation from a deeper surface. In the case of the  $0.05^\circ$  scan, the ratio for the Se flux of 35 Å/s is 2.4, while that for the Se flux of 15 Å/s Se is 5. The results show that the orientation preference

is fully lost at the surface of the CIGS film for both conditions.

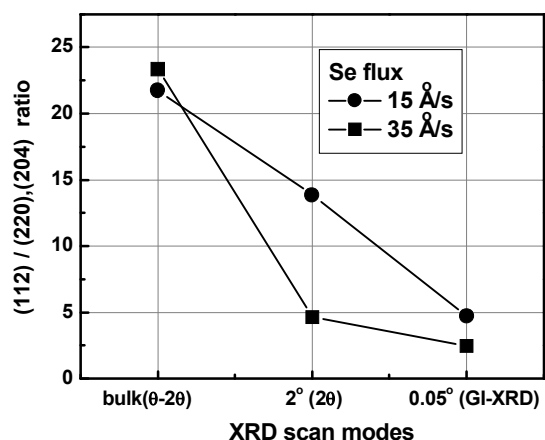


**Fig. 3.** Intensity ratio of (112)/(220)/(204) in CIGS films taken with various XRD incident angles: bulk ( $\theta - 2\theta$  scan),  $2^\circ$  ( $2\theta$  scan), and  $0.05^\circ$  (GI-XRD).

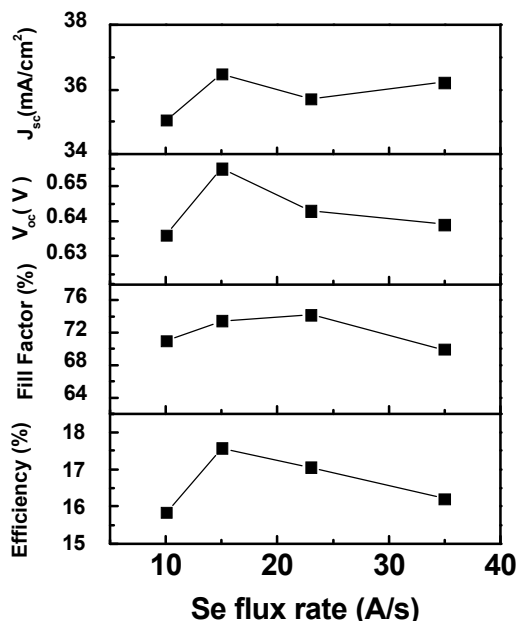


**Fig. 4.** Photovoltaic parameters of CIGS solar cell as a function of Se flux under AM 1.5 illumination.

Figure 4 shows photovoltaic parameters as a function of Se flux. For the Se flux of 35 Å/s, the open circuit voltage and fill factor are reduced. It is considered that the distinctive reason comes from the formation of pores on surface. After CdS buffer layer deposition, there is a lot of poor CdS/CIGS region since the pores on

CIGS surface is too deep to be uniformly deposited by CdS buffer layer. Therefore, the CIGS solar cell with 35 Å/s Se flux shows poor diode quality factor and series resistance as  $\sim 2.01$  and  $\sim 0.51 \Omega\text{cm}^2$ . Until so far, it is reported that strong (220)/(204) texturing is essential to get high efficiency[1]. However, in our study, the growth of (220)/(204) plane in strong (112) CIGS film makes pores on surface and poor diode ideality factor, so poor photovoltaic properties can be obtained. It means that partial growth of (220)/(204) plane among (112) planes does not help improvement of high efficiency CIGS solar cells. when the Se flux is less than 15 Å/s, cell data also show over all lower performance. It is considered that insufficiency of Se flux during CIGS deposition make the quality of film poor. Especially, the cell shows poor shunting resistance as  $\sim 470 \Omega\text{cm}^2$ . Consequently, Se flux during CIGS deposition critically determines these behaviors on photovoltaic properties. For the Se flux of 15 Å/s, CIGS solar cells shows the best performance and strong (112) preferred orientation.

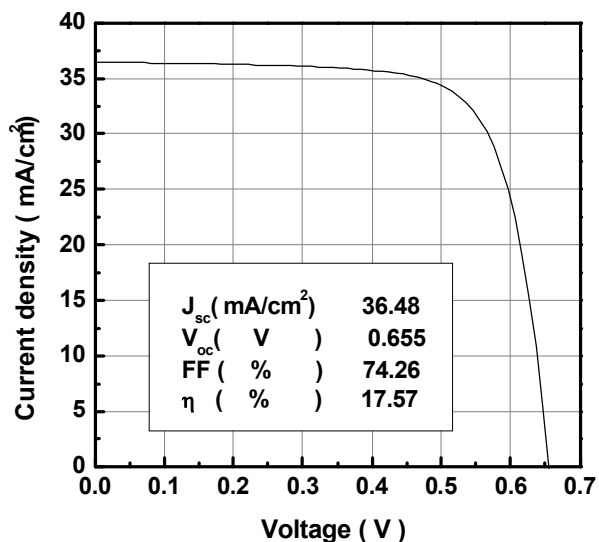


**Fig. 5.** Illuminated J-V curve of the CIGS solar cell under Se flux of 15 Å/s.

Figure 5 shows the J-V curve of the best cell, which has a conversion efficiency of 17.57% with  $J_{sc} = 36.48 \text{ mA/cm}^2$ ,  $V_{oc} = 0.655 \text{ V}$ , and  $FF = 73.52\%$  in an active area of  $0.421 \text{ cm}^2$ . The diode quality factor and series resistance are  $1.62$  and  $0.26 \Omega\text{cm}^2$ , respectively.

## CONCLUSIONS

The CIGS film was deposited the “three stage process” co-evaporation and the influence of Se flux on CIGS solar cell was dealt with in this article. Se flux had

great influence on the microstructure and morphology of CIGS layer during the third stage. The pores were developed on CIGS surface with 35 Å/s Se flux condition and it is considered that formation of pores is caused by long range diffusion through liquid  $\text{Cu}_{2-x}\text{Se}$  phase during the third stage. Moreover, (220)/(204) planes beside (112) plane was developed near CIGS surface. However, with Se flux of 15 Å/s, the CIGS surface showed tightly connected structure and the pores on surface were removed. At this condition, The best CIGS solar cell showed the conversion efficiency of 17.57% with  $J_{sc} = 36.48 \text{ mA/cm}^2$ ,  $V_{oc} = 0.655 \text{ V}$  and  $FF = 73.52\%$  in an active area of  $0.421 \text{ cm}^2$ . The adjustment of Se flux was essential parameter to get better micro-structure and also photovoltaic properties. More details can be found in the literature[10].

## REFERENCES

- [1] M.A. Contreras, K. Ramanathan, J. AbuShanma, F. Hasoon, , D. L. Young, B. Egaas, and R. Noufi, "Diode Characteristics in State-of-the-Art  $\text{ZnO/CdS/Cu(In}_{1-x}\text{Ga}_x\text{)Se}_2$  Solar Cells", *Prog. Photovolt. Res. Appl.*, **13**, 2005, pp. 209-216.
- [2] M. Nishitani, T. Negami, and T. Wada, "Composition Monitoring Method in  $\text{CuInSe}_2$  Thin Film Preparation ", *Thin Solid Films*, **258**, 1995, pp. 313-316.
- [3] S. Chaisitsak, A. Yamada, and M. Konagai, "Preferred Orientation Control of  $\text{Cu(In}_{1-x}\text{Ga}_x\text{)Se}_2$  ( $x \approx 0.28$ ) Thin Films and Its Influence on Solar Cell Characteristics", *Jpn. J. Appl. Phys.*, **41**, 2002, pp. 507-513.
- [4] S. H. Kwon, B. T. Ahn, S. K. Kim, K. H. Yoon, and J. Song, "Growth of  $\text{CuIn}_3\text{Se}_5$  Layer on  $\text{CuInSe}_2$  Films and its Effect on the Photovoltaic Properties of  $\text{In}_2\text{Se}_3/\text{CuInSe}_2$  Solar Cells", *Thin Solid Films*, **323**, 1998, pp. 265-269.
- [5] D. Y. Lee, J. H. Yun, K. H. Yoon, B. T. Ahn, " Characterization of Cu-poor surface on Cu-rich  $\text{CuInSe}_2$  film Prepared by Evaporating Binary Selenide Compounds and Its Effect on Solar Efficiency ", *Thin Solid Films*, **410**, 2001, pp. 171-176.
- [6] J. R. Tuttle, M. Contreras, M. H. Bode, D. Niles, D. S Albin, R. Matson, A. M. Gabor, A. Tennant, A. Duda, and R. Noufi, "Structure, Chemistry, and Growth Mechanisms of Photovoltaic Quality Thin-film  $\text{Cu(In,Ga)Se}_2$  grown from a Mixed-phase Precursor", *J. Appl. Phys.*, **77(1)**, 1995, pp. 153-161.
- [7] T. Walter and H. W. Schock, "Crystal Growth and Diffusion in  $\text{Cu(In, Ga)Se}_2$  Chalcopyrite Thin Films ", *Thin Solid Films*, **224**, 1993, pp 74-81.
- [8] T. Wada, N. Kohara, T. Negami, and M. Nishitani, "Growth of  $\text{CuInSe}_2$  Crystals in Cu-rich Cu-In-Se Thin Films", *J. Mater. Res.*, **12(6)**, 1997, pp. 1456-1462
- [9] J. Kessler, C. Chityuttakan, J. Lu, J. Schöldström, and L. Stolt, "Cu(In,Ga)Se<sub>2</sub> Thin Films Grown with a Cu-poor/rich/poor Sequence: Growth Model and Structural Considerations", *Prog. Photovolt. Res. Appl.*, **11**, 2003, pp. 319-331.
- [10] K.H. Kim, K.H. Yoon, J.H. Yun, and B.T. Ahn, "Effect of Se Flux on the Microstructure of  $\text{Cu(In,Ga)Se}_2$  Thin Film Deposited by Three-stage Co-evaporation Process", *Electrochem. Solid-State Lett.*, **9(8)**, 2006, pp. A382-A385